NASA TECHNICAL MEMORANDUM

NASA TM X-52937

ACOUSTIC PROPERTIES OF A SUPERSONIC FAN

by A. W. Goldstein, F. W. Glaser and J. W. Coats
Lewis Research Center
Cleveland, Ohio

TECHNICAL PAPER proposed for presentation at
Ninth Aerospace Sciences Meeting sponsored by the
American Institute of Aeronautics and Astronautics
New York, New York, January 25-27, 1971

ACOUSTIC PROPERTIES OF A SUPERSONIC FAN

Arthur W. Goldstein, Research Engineer, Frederick W. Glaser, Research Engineer,
and James W. Coats, Research Engineer
National Aeronautics and Space Administration
Lewis Research Center
Cleveland, Ohio

Abstract

An experimental study was made of the acoustics of a supersonic fan of short blade span. Measurements were obtained with and without stator blades (outlet guide vanes) to provide control of wake-chopping and other blade row interference effects. Both internal and external measurements show a relation between the internal shock-wave configuration and the intensity of the radiated sound.

Substantial variations in the flow conditions at each blade of a homogeneous blade row provides an obvious source of the observed pure tone system based on multiples of the rotational speed of the shaft. This pure tone system is in evidence internally at subsonic and supersonic rotor speeds but propagates substantial amounts of power externally only at supersonic rotor speeds.

E-6076

Symbols

a	sonic speed
c_a	active, or lifting portion of blade chord
k	integer, order of harmonic of van system
m	order of azimuthal mode - number of lobes in rotating pressure pattern
M	Mach number of flow relative to rotor
M_x	axial component of Mach number
n	order of roter frequency harmonic
N	rotational speed of rotor
p	pressure of gas
R	effective radius of fan annulus
R_g	gas constant
S	pitch of rotor blading
T	gas temperature
U	rotor linear speed
V	number of stator vanes
V_x	axial component of gas velocity
x	axial distance from rotor face
α	pitch angle, chord line to fan rotation axis
γ	ratio of specific heat of gas
ΔH_T	rise in stagnation enthalpy (specific) of gas passing through the fan
Δp	rise in static pressure from in flow to region on blade behind reflected loading shock
ΔT_T	rise in stagnation temperature of gas passing through fan
ρ	gas density
θ	shock wave angle to flow vector

Subscript T - stagnation condition

Introduction

The fan component of turbofan engines is a principle source of noise. This noise can be reduced by several design features including low fan trip speed and low gas velocity relative to the blades; reduction is achieved in both noise generation, and in the transmission of discrete tones through the fan ducting. Low speed fans, however, require drive turbines that have many stages and are relatively heavy.

In a proposed alternate design of a low noise fan, the fan blades move at supersonic speeds relative to the air, but the blades are designed in a novel way to minimize wave propagation, upstream. Waves propagated downstream can be absorbed by acoustic baffles. Elimination of the upstream baffling will reduce interference with the rotor inflow, and also the noise generated by the rotor. The drive turbine required for this high speed fan will have one or two stages and be light in weight.

This paper presents the experimentally obtained acoustic characteristics of a research fan, designed to eliminate the forward propagation of pressure waves, and some related aerodynamic characteristics.

Aerodynamic Design

Wave System

The high speed fan of the transonic type is in common use, and operates with the rotor blade tips moving at supersonic speeds relative to the gas, and the blade roots moving at subsonic relative speeds. There is an intermediate section of the blade operating at such a low supersonic speed that normal bow waves extend across the leading edge of the blade, the adjacent interblade channel and upstream (fig. 1). This pattern persists to the very tip, and results in efficient compression and high work input.

To eliminate the upstream waves, the rotor blades were designed with a sharp leading edge, and a trailing (suction) surface with sufficiently long straight section, that any pressure wave originating on the surface is intercepted by the following blade. Without such waves traveling upstream from the blade surface, the subsonic axial velocity is adjusted by disturbances from the leading edge so that the air approaches the blade parallel to the trailing surface of the blade, and thereby eliminates the upstream moving branch of the bow wave. The gas is deflected through the wedge angle on the leading side of the blade by a downstream shock wave (see fig. 2).

A second feature of the design insures that the detached normal shocks become attached oblique shocks when the rotor speed is sufficiently high; the solidity of the blading is sufficiently low that interblade channels are eliminated, and the possibility of choking flow in blade channels is avoided.

The attainment of gas compression without detached bow waves is provided by a system of waves originating on the trailing edges of the blades. A pressure wave travels upstream and is intercepted and reflected downstream by the following blade (see fig. 4).

The pressure rise through these shocks provides the aerodynamic loading. The flow direction of this air passing over the the following surface has been altered by the terminal shock wave. The flow from the leading surface is equally deflected by an expansion wave traveling downstream from the trailing edge. The complete wave system is shown in Fig. 2. Figure 3 shows the waves which result from the blade shape, and Fig. 4 shows that portion related to the blade loading. If the terminal shock is made sufficiently strong, a normal shock impinges on the following blade, rather than an oblique shock. The normal terminal shock provides an upper bound to the blade loading; it is not a satisfactory operating condition because of fluctuation of the wave location, and forward noise propagation.

Estimated Capacity

The aerodynamic loading of which the blades are capable may be estimated from the wave system. If the thickness of the blade is altogether ignored for a rough estimate, and if we suppose the blade to be uncambered, then the trailing edge shock wave with wave angle θ_W will impinge on the following blade at a point from which the distance to the trailing edge is c_a. This portion of the thin, uncambered blade is the only section which is loaded; let the pressure rise produced by the wave be Δp, and the pitch angle (chord line to fan rotation axis) be α. Then

$$c_a = -S \cos(\theta_W + \alpha)/\sin\theta_W$$

where S is the tangential spacing of the blade. The tangential force on the blade is then

$$c_a \Delta p \cos\alpha$$

and the rate of work on the gas is

$$Uc_a \Delta p \cos\alpha$$

where U is the rotor linear speed. The mass flow through the rotor per rotor blade is

$$\rho V_x S$$

where

ρ gas density
V_x axial component of gas velocity

Thus the work input per unit mass, or rise in stagnation enthalpy is

$$\Delta H_T = [Uc_a \Delta p \cos\alpha]/[S\rho V_x]$$

$$= -[\cos(\theta_W + \alpha)\, UR_g T \Delta p \cos\alpha]/[\rho V_x \sin\theta_W]$$

where R_g gas constant, T gas temperature. For the special case of zero prerotation, $U = V_x \tan\alpha$

$$T = T_T/[1 + (\gamma - 1)M_x^2/2]$$

$$M_x \equiv M \cos\alpha$$

where γ, ratio of specific heats, subscript T indicates stagnation condition, and there is obtained for the temperature rise ratio

$$\Delta T_T/T_T = -[(\gamma - 1)/\gamma][\Delta p/p] \sin\alpha \cos(\theta_W + \alpha)/$$
$$\sin\theta_W (1 + (\gamma - 1)M_x^2/2)$$

For assumed conditions of $M = 1.6$ and $M_x = 0.6$ and an adiabatic efficiency of 85 percent, a normal shock configuration would produce a fan pressure ratio of about 3.0. The normal shock is somewhat excessive because of the tendency of such a shock to oscillate in front of and behind the following blade as flow conditions fluctuate, giving rise to large noise propagation frontwards. A very conservative limit would be one in which the Mach number is 1.0 after the reflected wave. Here the achievable pressure ratio would be 1.65. From these estimates it appears that a fan of this type can develop pressure ratios of interest for applications.

Fan Test Rig

An overall view of the fan is shown in the photograph of Fig. 5, and additional details in the sectional view of Fig. 6. The test rig is designed so that no supports project into the internal airstream. The front fairing, the outside casing, and the combination of rotor bearings and internal casing are all supported independently from the test bed. The driving power was provided by an air turbine driven by the service air supply.

The rotor was 18 in. (45.7 cm) in diameter at the blade tips, and 16 in. (40.65 cm) at the roots. Other significant dimensions are shown in Fig. 7. The blade sections shown are the same for all radial sections (straight, untwisted blade). There were 26 rotor blades. At 2.59 in. (6.58 cm) downstream of the rotor was a stator assembly of 69 blades; this stator was removed for testing of the rotor alone. In front of the rotor was an annular cylindrical duct containing acoustic measuring stations located at the following distances upstream of the rotor - 0.42 in (1.07 cm), 2.38 in. (6.04 cm) and 4.38 in. (11.12 cm). There was an additional station located at the stator discharge 3.51 in (8.92 cm) behind the rotor blade trailing edges. The front cylindrical section was blended into a bell-mouthed intake at 4.38 in. (11.12 cm) upstream of the rotor face (fig. 6).

From the dimensions of the rotor it was calculated that at zero angle of attack on the rotor blades, relative velocity of approach to the blade tips was equal to sonic speed at 13,700 rpm (std. inlet condition); Mach number of 1.0 at the roots was attained at 15,200 rpm. Because of expansion waves emanating from the trailing surface of the blades which increased the Mach number ahead of the leading edges, it was estimated that attached bow waves were achieved at those speeds. Interception of the expansion wave and downstream progression of the

bow wave was estimated to have been achieved at 19,200 rpm at the blade roots, and at 19,700 rpm at the blade tips.

The fan rig was operated in an outdoor environment. Acoustic measurements in the far field were made at a distance of 12.5 feet (3.81 m) from the rotor; additional internal measuring stations have been described. Analysis of acoustic data into 1/3 octave band pass spectra was done on line or from magnetic tape records. This analyzer had an approximate time constant of 3 seconds. A longer time constant would have been desirable; consequently, 3 samples were obtained for each condition. Narrow band spectral analysis was also used with 10 Hz band-widths. All sound pressure levels were referenced with respect to 0.0002 microbar.

Aerodynamic measurements were made at a time other than when acoustic measurements were made in order to avoid interference of the instrumentation with the fan noise. Nine thermocouples surveyed the air temperature just inside the bellmouth. Three static pressure taps and atmospheric pressure provided mass flow data. Downstream total pressure and total temperature rakes were located just behind the stator.

Aerodynamic Performance

Overall Performance

The aerodynamic performance of the fan is shown in Fig. 8. The desired gas flow was attained. Consequently we have some assurance that the desired wave configuration was achieved at the mean span position. The efficiencies obtained at high speed are too low for direct use of this design, and two possible reasons are presented. First, the blades could not be loaded adewuately by closing down the back throttle because of the limited power available from the driving turbine at 70 percent of design speed and higher. Diffusion factor of the blading was only 0.1, whereas values of 0.5 to 0.6 are often used in practice. As a result, energy losses occur in the fan which are a large percentage of the energy input to the gas, and the efficiency is low. Secondly, the blades were designed with a short span to approximate a two-dimensional flow. The short span of the blades results in relatively important end losses, which are generally much higher than mid-span losses.

Rotor Pressure Field

The variation of pressure with time at a close upstream location, 1 cm from the rotor face was expected to give an indication of the wave system. A series of oscilloscope traces of these data are shown in Fig. 9. As the rotor speed increases from low supersonic speeds to high supersonic speeds, the pressure amplitude increases and then falls off. Although these data are not suitable for detailed amplitude calculation because of the extreme and unexpected variability of the pressure and flow from one blade space to the next, some characteristics can be noted. Two traces obtained at different azimuthal stations during rotor operation at 15,000 rpm, indicate pressure fluctuations as much as 0.25 psi (1723 N/m^2). At this speed the rotor is operating in barely supersonic flow, and pressure waves should be propagating forward. Especially noteworthy is the irregularity of the waves at one of the measuring stations. Such irregularities are the obvious cause for rotor harmonic tones which show up in the spectrum of the noise. At 18,000 rpm the calculations indicate that the transfer of the waves from the front to the back should be occuring; the pressure trace shows that this process proceeds more completely for some blades than others. The rotor harmonics should be relatively prominent in the spectrum of this noise. At 19,400 rpm the trace clearly shows a blade passing tone, although it was expected that this would not be present if the bow wave were transferred from the front of the cascade to the rear, as planned. The fact that a substantial level of pressure fluctuation exists may be ascribed to the lack of twist of these blades.

At 18,000 rpm, at the mean radius of 8.515 in. (21.62 cm) the rotor speed is 1260 ft/sec (320 m/sec). Since the blade stagger angle is 73°, the axial velocity is 411.6 ft/sec (104.5 m/sec). With this value for V_x, the rotor speed at the tip results in a relative gas flow angle of $73^\circ\ 46'$ and at the hub of 72°. The blade angle is the same at all locations, and the resultant angle of attack is -1.0° at the hub and $+0.75^\circ$ at the tip. At the hub the Mach number is 1.205, and the compression wave radiating from the leading edge causes a rise in pressure of 5.3 percent, or 0.71 psi (4900 N/m^2). Compression at the blade tips is 0.57 psi (3930 N/m^2). The size of the opening to the instruments and the limitations of the amplifying system do not permit a good sharp wave form to be exhibited, so one can expect only the first few harmonics of the wave to show. The fundamentals of the saw-tooth waves of the above amplitudes would be 0.45 psi (3120 N/m^2) at the hub and 0.36 psi (2500 N/m^2) at the tips. There will be a further reduction in amplitude because of interaction of the waves from the blade roots and tips. The pressure readings were about 0.16 psi (1103 N/m^2) on the average, so that this mechanism is adequate to generate the pressures observed. Incorporation of blade twist into the blade design may substantially reduce the level of front radiation from the rotor.

Acoustic Performance

Sound Spectrum Produced

Spectrograms of the noise produced by the rotor, and measured at the station 1 cm upstream are displayed in Fig. 10. The spectrum at low speed (10,300 rpm) is seen to possess a blade passing tone and a series of discrete tones, all harmonics of the shaft speed. These tones have been previously reported as having been observed only at supersonic flow conditions [1, 2, 3]. Mather, Savidge, and Fisher have observed such tones in the far acoustic field of a rotor turning at subsonic speeds (fig. 4(a) of ref. 4). (Their paper is not clear on whether or not the rotor had sufficient housing to dampen these rotor tones.) The presence of the tones at low speed indicates that they result from azimuthal pressure distributions which are not identical from one

blade space to the next. This non-periodic character was demonstrated in the pressure-time traces of Fig. 9. At 14, 300 rpm, the outer annulus of the rotor is operating at supersonic speed; the spectrogram for this case shows a higher level of the rotor harmonic tones.

At 18, 500 rpm (fig. 10(c)) the blade passing tone is still present; the shaft harmonic tones are about the same magnitude as for the barely supersonic case. The root-tip pressure waves resulting from the angle of attack on the untwisted blade produce a sound pressure level from the fundamental frequency which may be estimated by assuming an average pressure deviation for the hub and tip blade sections of 0. 41 psi (2810 N/m^2). (Peak to peak, also see previous calculations.) Reduction to rms value gives 993 N/m^2. If one assumes a linear variation of this pressure from root to tip, the power-averaged rms pressure is

$$993/\sqrt{3} = 573\ N/m^2$$

or a sound pressure level of 149. 2 db. Time-averaged data, presented in Fig. 14 is 148 db. Therefore this theory of pressure waves emanating from the blade tips and roots will account for the observed noise. The conclusion to be drawn, is that for supersonic blades of this type, the elimination of blade passing tone requires very precise distribution radially, of the blade stagger angle. The passage of a normal shock wave would give a pressure rise of 6. 6 psi (45, 000 N/m^2) at the blade root Mach number of 1. 19 and of 12. 6 psi (87, 000 N/m^2) at the blade tip Mach number of 1. 34. If attached bow waves of 6^o deflection strength existed at the blade tip, the pressure rise at the tip would be 5. 1 psi (35, 000 N/m^2). The actual pressure rise is so much less than these shock waves would cause, and in such close agreement with fluctuations originating in misalignment, that one may conclude the front-radiating waves have indeed been deflected into a rear-radiating wave system as planned.

Transmission of Pressure Waves

Not all the pressure disturbances produced by the rotor will propagate through the annulus or into the far field. Therefore the spectrograms will differ at the several stations. At subsonic speeds, sound transmission is indicated by comparison of the spectrograms for 10, 300 rpm at stations (1) just upstream (1. 1 cm) of the rotor face (fig. 11(a)), (2) 11. 1 cm upstream face (fig. 11(b)), and (3) in the far field 3. 81 m from the rotor at an angle of 30^o from the inflow direction (fig. 11(c)). There is no internal attenuation of the broadband noise. (The broadband measurements in the far field are useless, since these levels are independent of fan speed and must therefore consist primarily of background noise.) The blade passage tone and shaft harmonics are both attenuated, which indicates that they are both spiralling waves. According to simple two-dimensional cartesian approximation, the decay rate in decibels per unit of axial length of the duct is equal to

$$\Delta/x = 8.69\ (m/R)\ \sqrt{1 - M^2}/[1 - M_x^2]$$

where m is the number of lobes of the mode around the axis (azimuthal order)

R the effective radius of the annulus

This result can be obtained by a coordinate transformation relative to the fluid, according to the method of Ref. 5.

From this equation it is clear that the shaft harmonics of low order (m small) will be transmitted more readily than the blade passing tone. At 10, 000 and 14, 000 rpm for the particular rotor under study, the decay to the station 11. 1 cm forward of the rotor is given in the table. The blade tone has 26 lobes.

Speed, rpm	m	1	2	4	8	16	26
10, 000	Δ (db)	3. 1	6. 1	12. 3	24. 5	49. 0	79. 7
	freq. (Hz)	167	333	667	1340	2670	4330
14, 000	freq. (Hz)	1. 1 233	2. 1 466	4. 3 933	8. 5 1860	17. 1 3730	27. 8 6060

Table I Decay of Various Modes in 10. 1 cm

For most of the important tones the decay rates are sufficiently high to prohibit external detection at the low operating speed. At the cut-off speed of 14, 300 rpm (fig. 12) the decreased decay predicted in the calculation is confirmed by the appearance of some of the rotor harmonic tones in the far field spectrum, while at the supersonic speed of 18, 300 rpm (fig. 13) these tones are readily transmitted to the far field, along with the blade passage tone. These rotor harmonics first become apparent in the far field at supersonic rotor speeds because of both the increased rate of generation by the rotor at supersonic speeds, and also because of improved transmission.

The transmission of the blade passing tone can be estimated from time-averaged sound levels given by the 1/3 octave band-pass analyzer. Corrections were made for background noise by estimations from adjacent filters. Where the blade tone affected two filters, the corrected levels were combined. The results are shown in Fig. 14. Noteworthy is the observed decay in the first 5 cm, and the absence of any decay thereafter. An estimate was made of the damping of the blade passing tone, and is shown in table II, compared with the measured rates.

N (rpm)	6, 000	8, 000	10, 000	12, 000	14, 000
Estimated (db)	48. 9	45. 4	39. 8	31. 3	13. 9
Measured (db)	23	25	28	29. 5	8

Table II Decay of Blade Passing Tone, 5. 1 cm

These data and estimates show that at subsonic speeds the blade passing tone decays within the first 5 cm or less, and there is subsequently transmitted a detectible

tone which does not attenuate; the transmitted wave must be either a spiralling wave rotating at supersonic speed, or a plane wave. Rotating blade stall could form such a wave. Stall is a likely possibility with rotor blades having sharp leading edges and operating in subsonic relative flow.

The blade passing tones at supersonic relative flow conditions (rotor speeds greater than 15, 200 rpm) do not decay in the annulus between the stations 1 cm upstream and 11 cm upstream of the rotor face. The attenuation of rotor shocks was calculated by Morfey and Fisher[6] for the interaction of a two-dimensional wave system of normal bow waves and expansion waves. Their calculation would predict a level of about 167 db at the closest station, 158 db at the 6 cm station, and 154 db at the farthest (11 cm). Our measured levels are much lower near the rotor face , and the predicted attenuation rates are not present. One can therefore conclude that the two-dimensional wave system resulting from detached shocks interacting with expansion waves has been eliminated in the blading of this rotor.

Figure 14 gives evidence that the desired wave system (fig. 2) was established. The amplitude of the blade passing tone at 1 cm ahead of the rotor increased with speed until 16, 200 rpm, above this speed there is a fall-off of 10 db at 18, 200 rpm, as would be expected if the upstream waves were transferred downstream. The downstream station, also as expected, has a higher sound level then the upstream station. Because the noise level at 18, 000 rpm is accounted for by the theory of pressure waves originating in flow attack angles at the blade roots and tips it is believed that this noise can be substantially reduced by twisting the blades properly. A similar plot of the blade passing tone sound pressure level at the two external stations, 40^{o} and 130^{o} from the front axis is shown in Fig. 15; the course of the data is similar to that at the entrance to the fan annulus, except for a loss of 34 db resulting from the increase in area from the internal station to that of a hemisphere of 3. 81 m radius.

Complete Fan Stage

The introduction of the outlet guide vanes of the stator, which redirects the rotor discharge flow from a spiralling to an axially directed flow will increase the noise level because of noise radiation from the stator vanes; these vanes intercept the rotor discharge wakes periodically, giving rise to interaction tones at the blade passing frequency. It is well known that these tones can be reduced to low levels by using large spacing between the blade rows. A different sort of interaction between the rotor frequency harmonics and the stators was described in Ref. 4, where evidence is presented to show that the order n (n = 1, 2, 3, $\cdots$) of the rotor frequency harmonic will determine the order m of the interaction tone by

$$m = n + kV$$

$k = 0, \pm 1, \pm 2, \cdots$ etc.

V = number of stator vanes

If $n = -V$, and $k = 1$, then $m = 0$, and a plane wave is formed which propagates at all rotative speeds. Our results with rotor alone indicates that for subsonic speeds the damping rate is large for such high order rotor tones, and that with wide axial spacing, this phenomenon should not be a serious problem. When the rotor is operating supersonically, it would seem that the separation would not reduce noise radiation because of the transmission of all rotor tones.

Noise was measured at an internal station just behind the trailing edges of the stator vanes and also at the station 11. 1 cm upstream. Sound pressure level of the blade passing tone is displayed in Fig. 16 at those two stations with and without the outlet guide vanes. The front end noise is essentially unchanged by the presence of the outlet vanes, either at subsonic or supersonic speeds.

Radiation rearwards is greatly increased by radiation from the vanes at subsonic speeds, but at supersonic speeds, the noise is decreased. The drop in sound pressure level at sonic speed (14, 000 rpm) measured at the downstream internal station, to a level below that for 12, 000 rpm indicates that the rotor blades wakes ceased to be an effective noise producer. At this speed and at higher speeds, the blade passing tone is reduced by the presence of the vanes. The vanes evidently do not radiate additional noise because of pressure fluctuations induced by shock wave impacts; they dissipate some of this sound energy.

Summary

The research fan showed a number of characteristics which indicate that the desired wave system was established at the blade mean section, whereby all pressure waves originating at the blade section were deflected downstream. These characteristics were:

1. Strong increase of noise with rotor speed as the relative gas velocity increased through sonic speed, indicating the inception of shock wave noise generation.

2. Transfer of noise radiation from frontwards to rearwards as thickness waves are reflected downstream, and the bow waves are transferred from upstream to downstream.

3. Residual front noise at high speed is approximately in agreement with the estimate from waves originating in slight misalignment of blade and gas flow over some portions of the blade span.

Also, noteworthy is the sharp cut-off of the blade passing tone as expected from the theory of propagating spiral waves; however, there appears to be an additional component of this tone which propagates undamped at all speeds even without the presence of outlet guide vanes.

Shaft harmonics are generated at subsonic speeds and are observable close to the rotor, contradicting the hypotheses of generation by non-uniformly generated shocks. They are subject to the same cut-off conditions

as the blade passing tone and therefore are usually observed in the far field of the fan with duct only at supersonic speeds.

A supersonic fan with blading designed for a wave system progressing downstream only may be feasible. Some secondary forward radiation in the research fan can most likely be eliminated with a refined design of the blade stagger angle.

References

1. Goldstein, A. W., Lucas, J. G., and Balombin, J. R., "Acoustic and Aerodynamic Performance of a 6-Foot Diameter Fan for Turbofan Engines, II Performance of QF-1 Fan in Nacelle Without Acoustic Suppression," TN D-6080, 1970, NASA, Cleveland, Ohio.

2. Ehrich, F. F., "Acoustic Resonance and Multiple Pure Tone Noise in Turbomachinery Inlets," Paper 69-GT-2, Mar. 69, ASME, New York, N. Y.

3. Kester, J. D. and Slaiby, T. G., "Designing the JT9D Engine to Meet Low Noise Requirements for Future Transports," Paper 670331, Apr. 1967, SAE, New York, N. Y.

4. Mather, J. S. B., Savidge, J., and Fisher, M. J., "New Observation on Tone Generation in Fans," Presented at Symposium on Aerodynamic Noise at the University of Loughborough, Sept. 1970.

5. Christensen, C. M., "The Sound Field of a Compressor Rotor," M. Sci. Thesis, M. I. T., June 1968.

6. Morfey, C. L. and Fisher, M. J., "Shock-Wave Radiation from a Supersonic Ducted Rotor," Aeronautical Journal, Vol. 74, No. 715, July 1970, pp. 579-585.

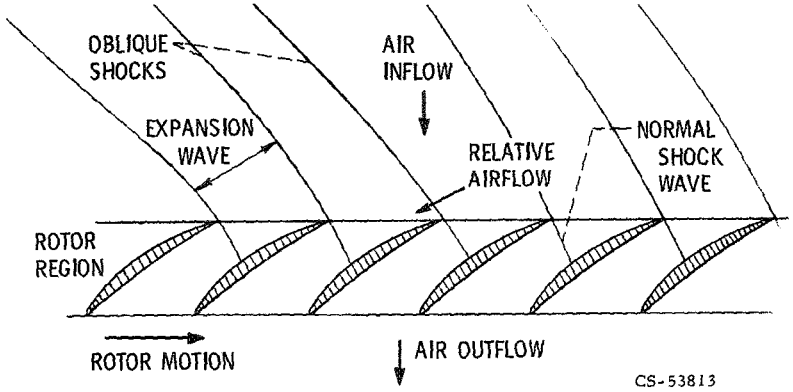

Figure 1. - Conventional design supersonic rotor blade sections.

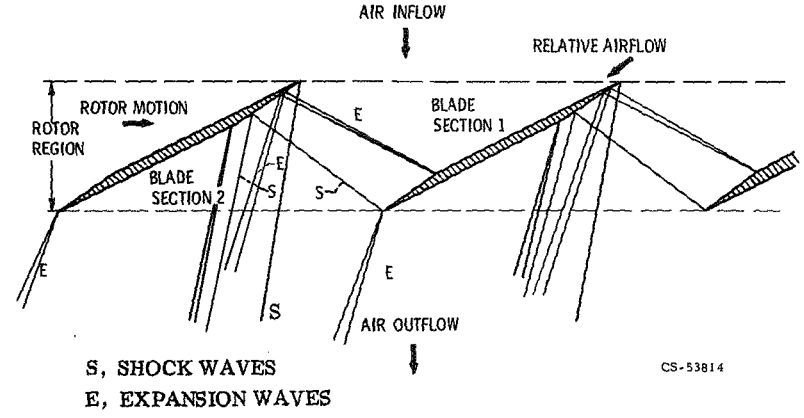

Figure 2. - Supersonic rotor blade sections - zero upstream disturbance.

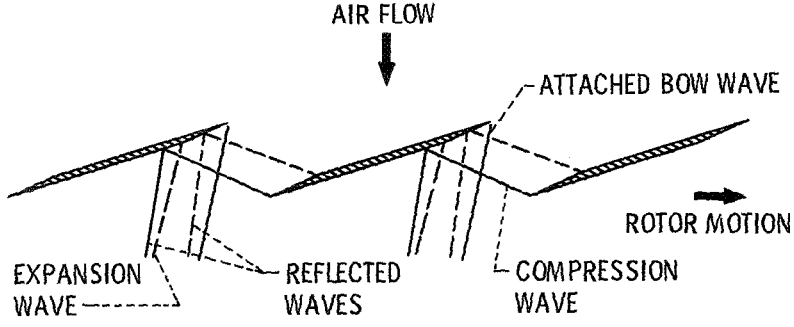

Figure 3. - Pressure waves resulting from blade thickness.

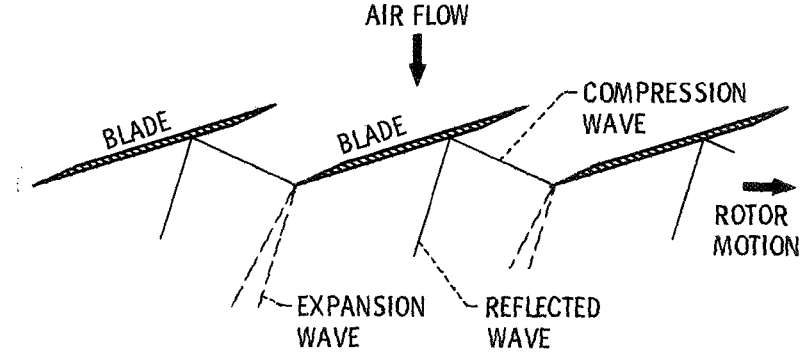

Figure 4. - Pressure waves resulting from blade loading (rotor back pressure).

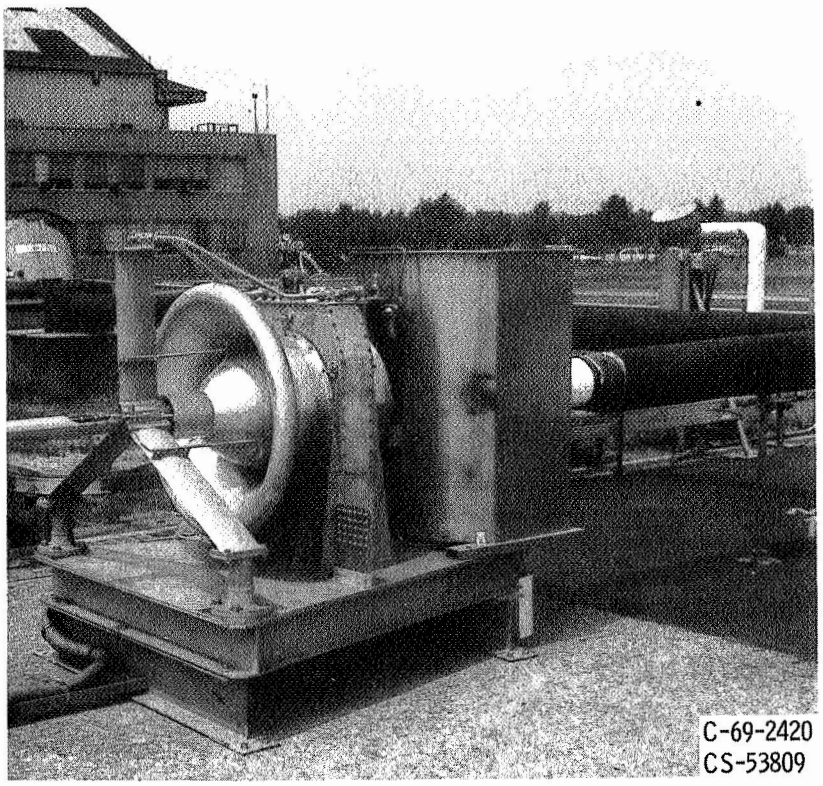

Figure 5. - Supersonic fan test rig.

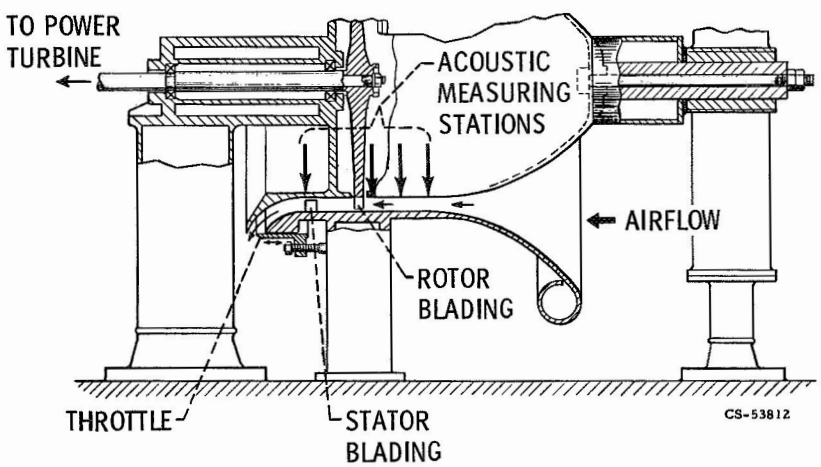

Figure 6. - Blade test with unobstructed flow path.

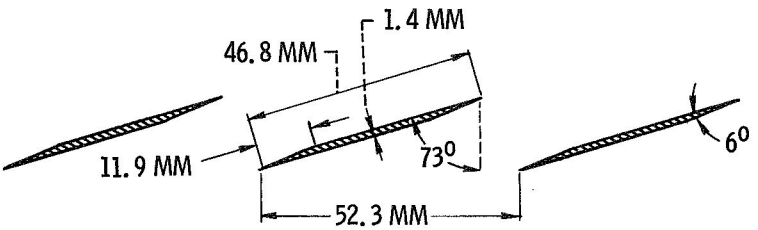

DIAMETER, TIP - 18 IN. (45.75 CM)
DIAMETER, HUB - 16 IN. (40.64 CM)
ROTOR SPEED - 20 000 RPM
ROTOR BLADE NO. - 26
STATOR BLADE NO. - 69
AXIAL SPACING - 2.6 IN. (6.61 CM)
RELATIVE GAS MACH NO. - 1.41
ROTOR BLADE DIFFUSION FACTOR - 0.10

Figure 7. - Fan design parameters.

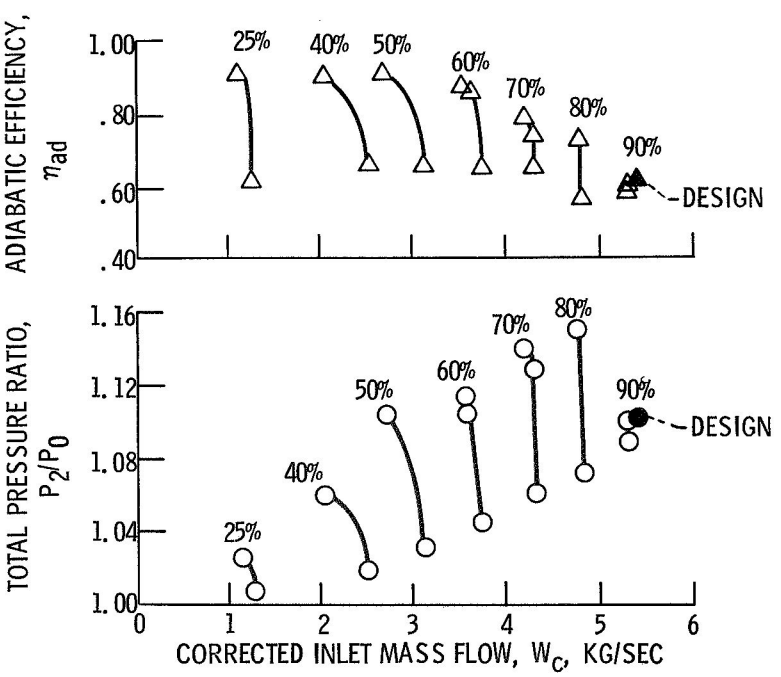

Figure 8. - Fan map.

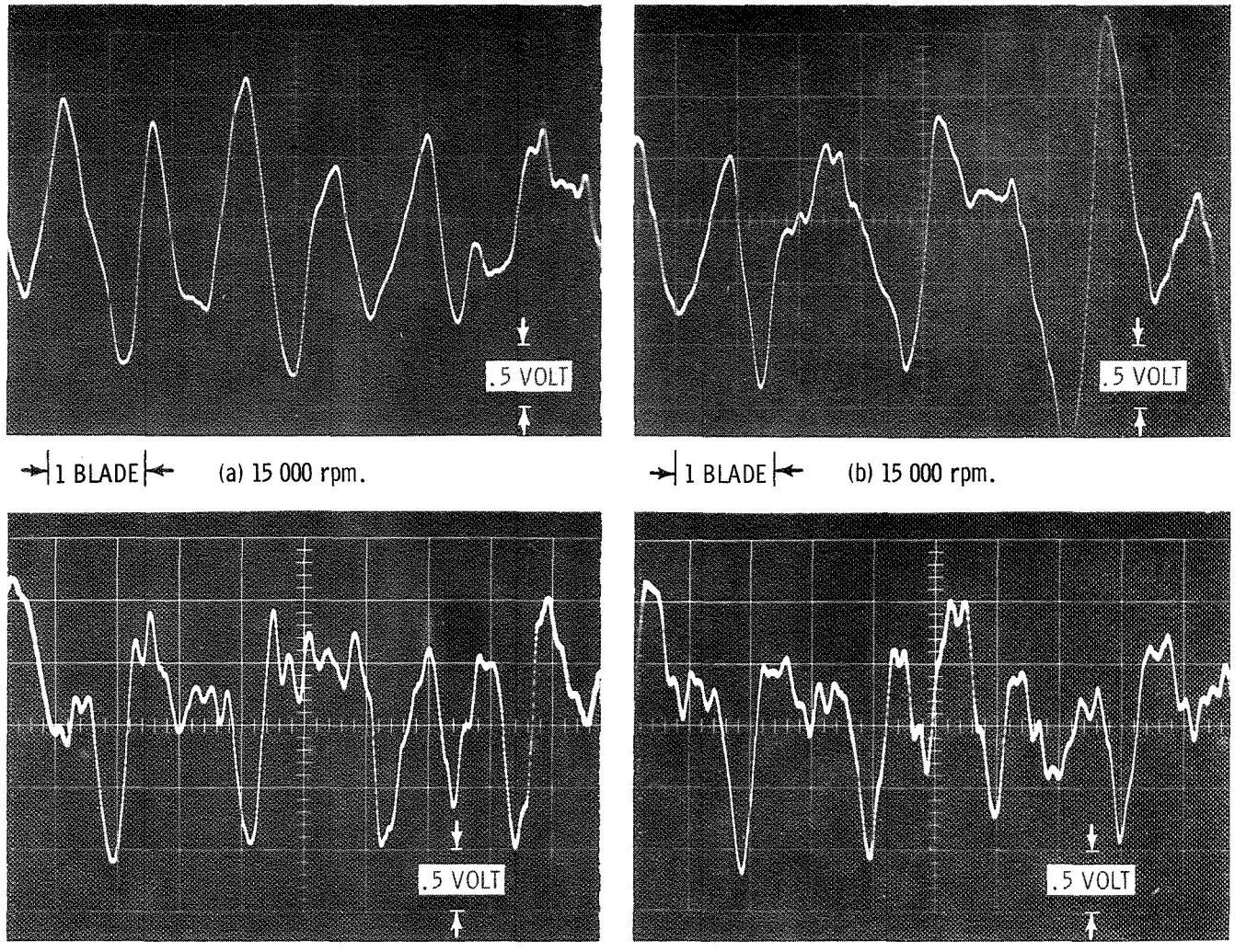

Figure 9. - Pressure - time history at rotor face.

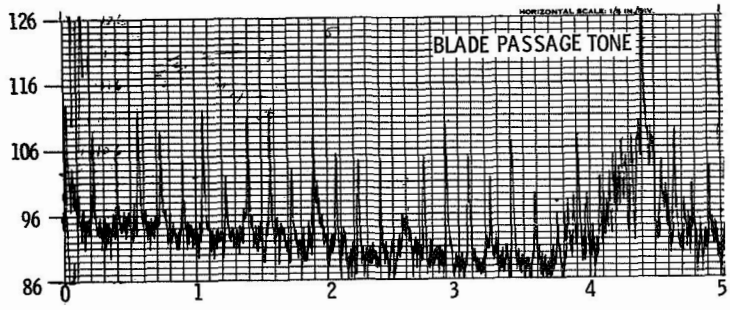

(A) 10 300 RPM.

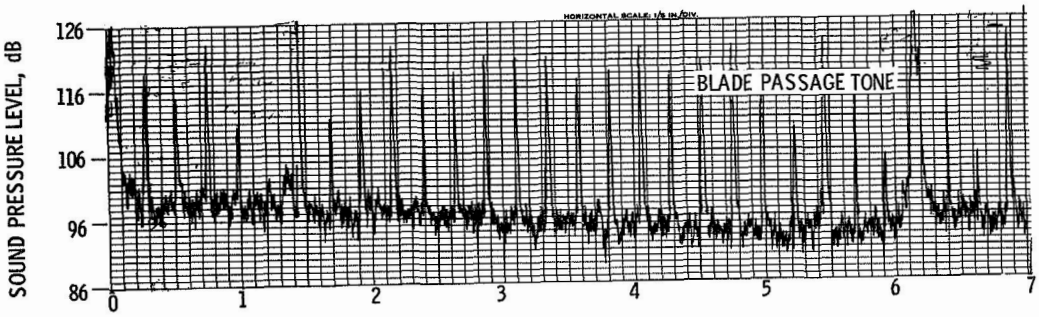

(B) 14 300 RPM.

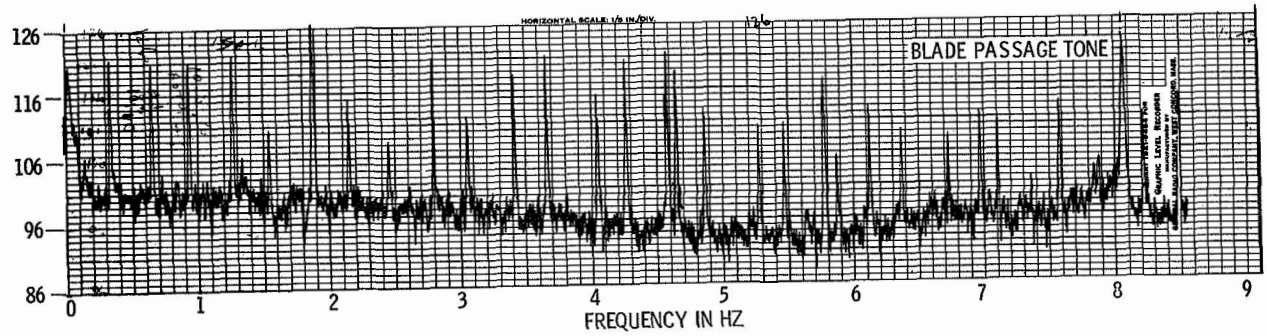

(C) 18 500 RPM.

Figure 10. - Spectrogram sound at rotor face.

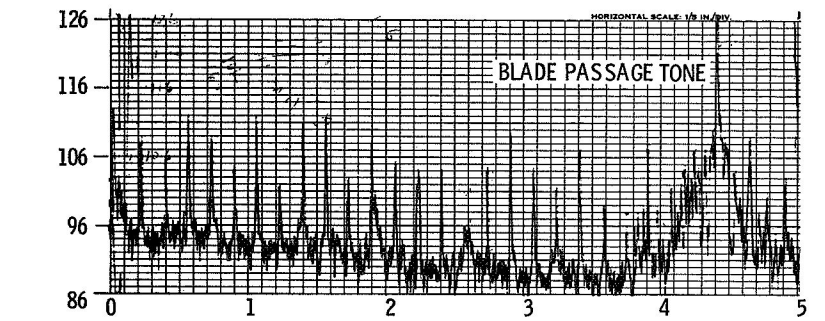

(A) STATION 1.

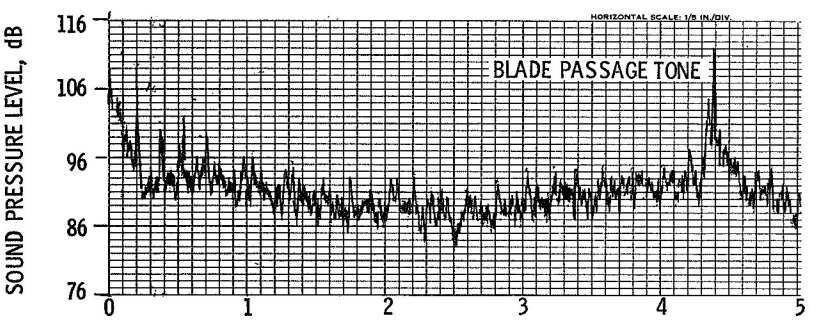

(B) STATION 2.

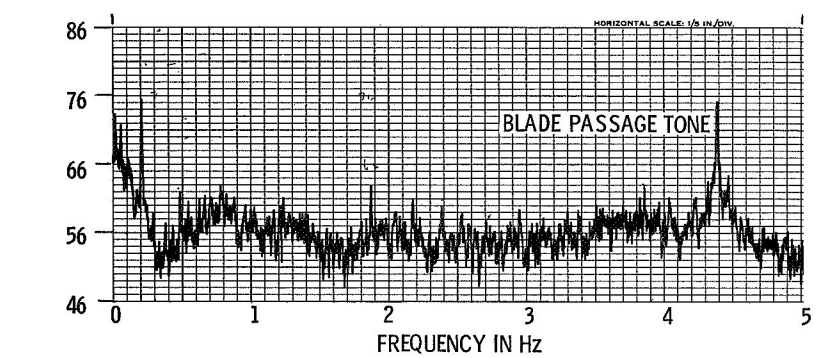

(C) STATION 3.

Figure 11. - Transmission of pressure waves. Subsonic speed 10 300 rpm.

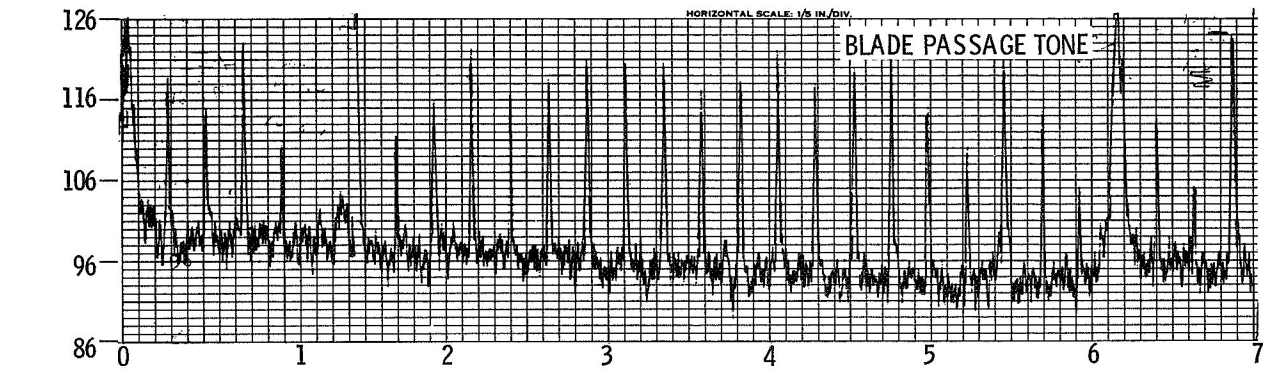

(A) STATION 1.

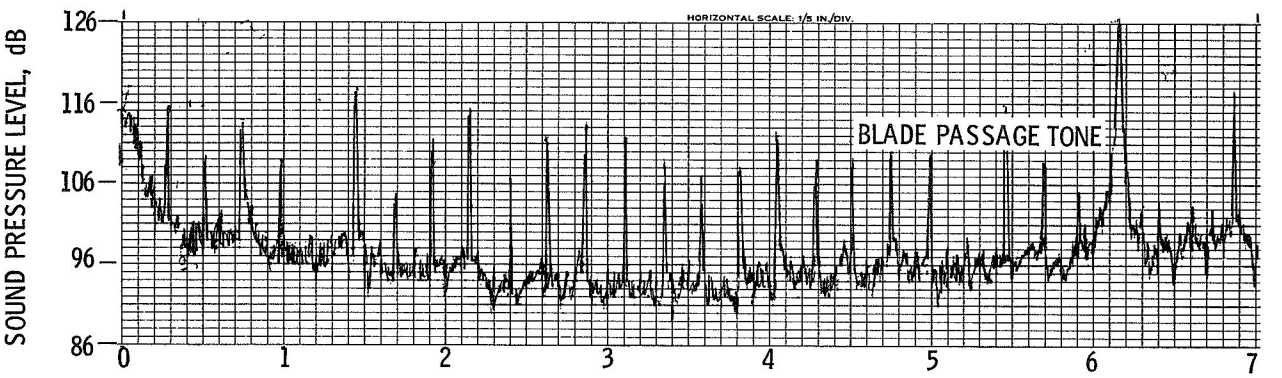

(B) STATION 2.

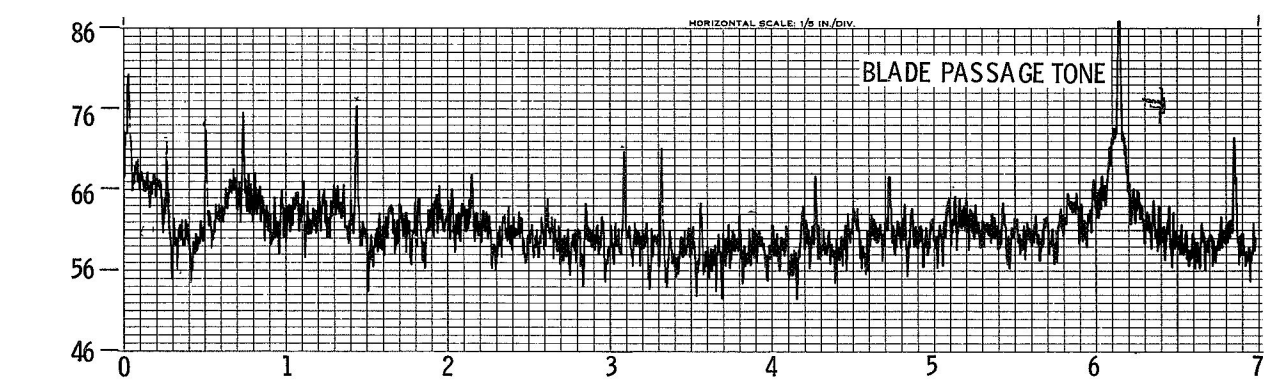

(C) STATION 3.

Figure 12. - Transmission of pressure wave sonic speed 14 300 rpm.

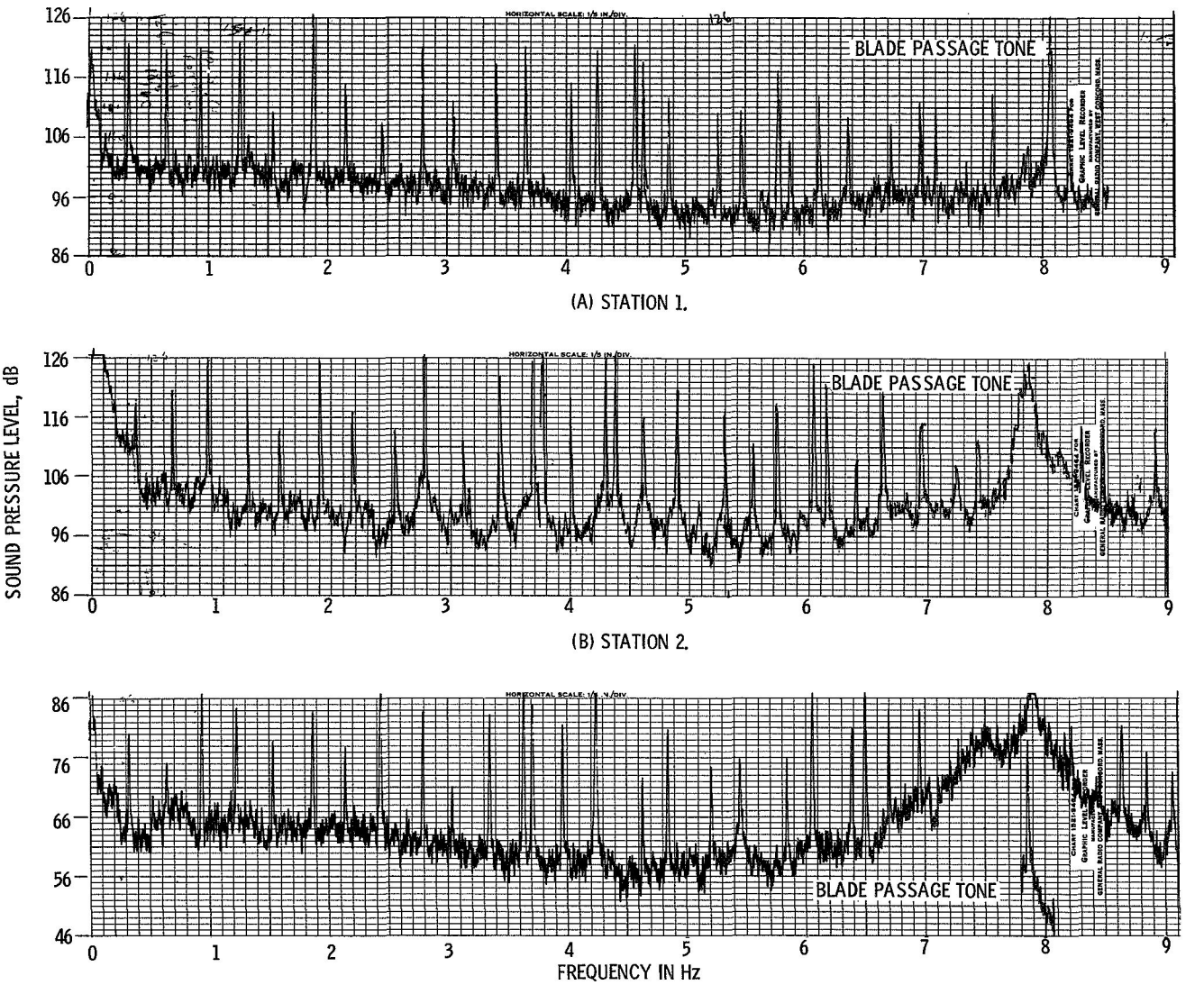

Figure 13. - Transmission of pressure waves supersonic speed 18 300 rpm.

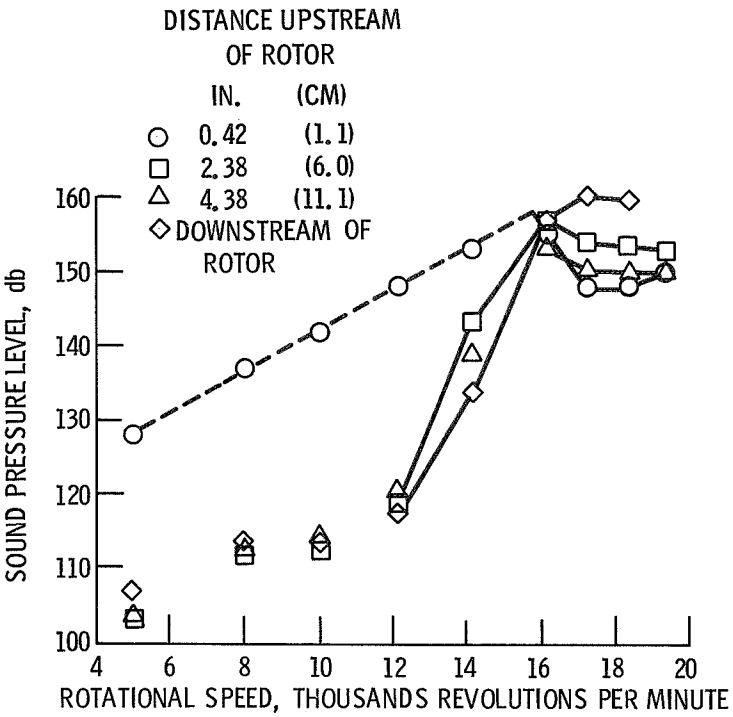

Figure 14. - Blade passing tone inside fan; rotor alone, open throttle.

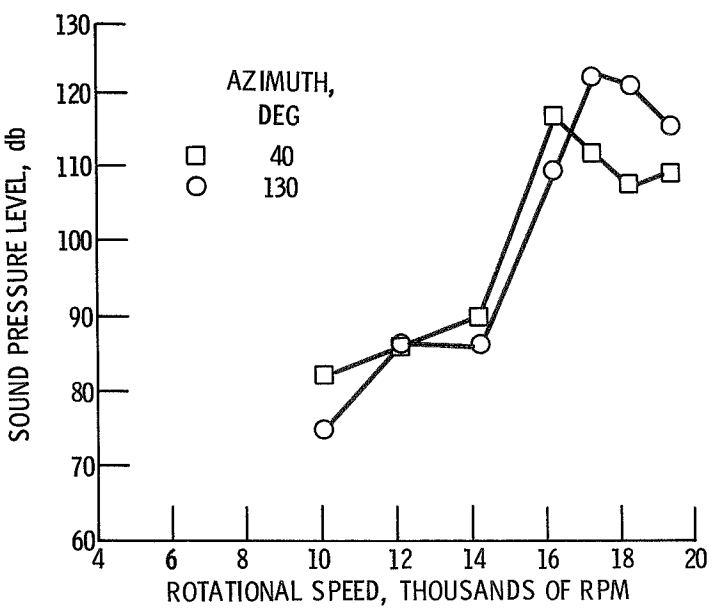

Figure 15. - Blade passing tone in far field; rotor alone, open throttle.

E-6076

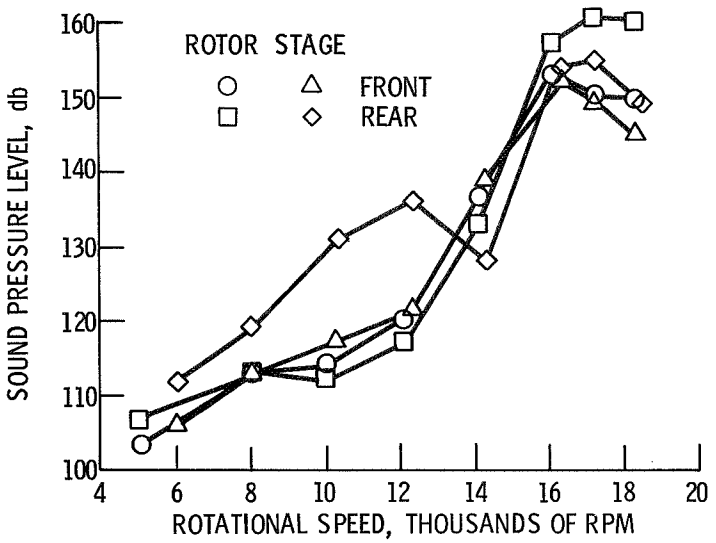

Figure 16. - Production of blade passing tone, comparison of rotor alone with complete stage.